



**UNIVERSIDADE ESTADUAL DE CAMPINAS
SISTEMA DE BIBLIOTECAS DA UNICAMP
REPOSITÓRIO DA PRODUÇÃO CIENTÍFICA E INTELECTUAL DA UNICAMP**

Versão do arquivo anexado / Version of attached file:

Versão do Editor / Published Version

Mais informações no site da editora / Further information on publisher's website:

<https://journals.aps.org/prl/abstract/10.1103/PhysRevLett.119.223002>

DOI: 10.1103/PhysRevLett.119.223002

Direitos autorais / Publisher's copyright statement:

©2017 by American Physical Society. All rights reserved.

DIRETORIA DE TRATAMENTO DA INFORMAÇÃO

Cidade Universitária Zeferino Vaz Barão Geraldo

CEP 13083-970 – Campinas SP

Fone: (19) 3521-6493

<http://www.repositorio.unicamp.br>

Ground-State Properties of Unitary Bosons: From Clusters to Matter

J. Carlson,^{1,*} S. Gandolfi,^{1,†} U. van Kolck,^{2,3,‡} and S. A. Vitiello^{4,§}

¹*Theoretical Division, Los Alamos National Laboratory, Los Alamos, New Mexico 87545, USA*

²*Institut de Physique Nucléaire, CNRS/IN2P3, Université Paris-Sud, Université Paris-Saclay, 91406 Orsay, France*

³*Department of Physics, University of Arizona, Tucson, Arizona 85721, USA*

⁴*Instituto de Física Gleb Wataghin, Universidade Estadual de Campinas, 13083-859 Campinas SP, Brazil*

(Received 26 July 2017; published 29 November 2017)

The properties of cold Bose gases at unitarity have been extensively investigated in the last few years both theoretically and experimentally. In this Letter we use a family of interactions tuned to two-body unitarity and very weak three-body binding to demonstrate the universal properties of both clusters and matter. We determine the universal properties of finite clusters up to 60 particles and, for the first time, explicitly demonstrate the saturation of energy and density with particle number and compare with bulk properties. At saturation in the bulk we determine the energy, density, two- and three-body contacts, and the condensate fraction. We find that uniform matter is more bound than three-body clusters by nearly 2 orders of magnitude, the two-body contact is very large in absolute terms, and yet the condensate fraction is also very large, greater than 90%. Equilibrium properties of these systems may be experimentally accessible through rapid quenching of weakly interacting boson superfluids.

DOI: 10.1103/PhysRevLett.119.223002

Introduction.—Strongly interacting fermionic cold atoms have been the subject of a great deal of study both theoretically and experimentally across the BEC to BCS transition, and especially at unitarity, where the two-body system has a nearly zero-energy bound state [1]. These systems are universal in that all properties, including ground-state energy, superfluid pairing gaps, superfluid transition temperatures, etc., are obtained as a set of universal dimensionless parameters multiplied by the Fermi energy or momentum of a free Fermi gas at the same density. Studies of bosonic superfluids, however, have concentrated on the weakly interacting regime described by the Gross-Pitaevski mean-field equation. These systems are comparatively simple to study as they were the first to be cooled to very low temperatures and their properties can be described in a mean-field picture.

It has been known for some time that short-range two- and three-body interactions can be used to describe the low-energy properties of small clusters of bosons. To obtain universal properties, the two-body interaction can similarly be taken to generate a zero-energy dimer, but a three-body interaction is required [2,3] to avoid the so-called “Thomas collapse” [4] of three or more particles. The resulting discrete scale invariance leads to geometric towers of states in systems with three [5] and more [6–10] bosons. Many atomic and nuclear few-body systems fall into this universality class [11].

In this Letter we demonstrate that large clusters and bulk matter are stable with such interactions, and similarly to the fermionic case described by a fairly simple set of universal parameters. We provide the first estimates for the universal parameters describing the ground-state energy, the equilibrium density, two- and three-body contacts, and

the condensate fraction of such a system. Our calculations are the analog of those carried out for fermions in Refs. [12,13], but here the universal parameters are directly related to the properties of the three-body system, i.e., its energy and radius. These bosonic universal properties may be accessible through cold-atom experiments, including those studying rapid quenching from weakly interacting Bose condensates.

Interaction and method.—The Hamiltonian we consider is

$$H = -\frac{\hbar^2}{2m} \sum_i \nabla_i^2 + \sum_{i<j} V_{ij} + \sum_{i<j<k} V_{ijk}, \quad (1)$$

where the first term is the nonrelativistic kinetic energy, the second the attractive short-range interaction tuned to infinite scattering length, and the last term is a repulsive three-body contact interaction tuned to produce a weakly bound trimer. For zero-range interactions universality has been demonstrated in Ref. [14]. For this study we employ finite-range two- and three-body interactions, keeping the range of these interactions much smaller than the size of the weakly bound trimer. For unitarity bosons this restriction is very stringent, as we shall see. The interaction must also be much shorter ranged than the average interparticle spacing in the bulk, which is an order of magnitude smaller than the three-body cluster size.

Here we employ Gaussian two- and three-body interactions:

$$V_{ij} = V_2^0 \frac{\hbar^2}{m} \mu_2^2 \exp[-(\mu_2 r_{ij})^2/2], \quad (2)$$

$$V_{ijk} = V_3^0 \frac{\hbar^2}{m} \left(\frac{\mu_3}{2} \right)^2 \exp[-(\mu_3 R_{ijk}/2)^2/2], \quad (3)$$

where $r_{ij} = r_i - r_j$ is the relative distance between bosons i and j , and $R_{ijk} = (r_{ij}^2 + r_{ik}^2 + r_{jk}^2)^{1/2}$. The strength V_2^0 is tuned to unitarity, and V_3^0 is tuned to reproduce a weakly bound three-particle state with a binding energy $-E_3$ and an associated radius $\bar{R}_3 \equiv (-2mE_3/\hbar^2)^{-1/2}$. The introduction of both two- and three-body range parameters $\mu_{2,3}$ allows us to produce arbitrarily weakly bound trimers for a given set of interaction ranges, which is essential to extract universal physics in the deeply bound many-body system.

Specific details of the interaction are not relevant as long as they are very short-ranged and the ground state can be tuned to a shallow trimer. In any physical system, the geometric tower of Efimov states at unitarity is truncated from below due to the range of the interaction. The binding energy of the would-be next deeper trimer is $\approx (22.7)^2$ larger than that of the calculated ground-state trimer; hence, the shape of our potentials should produce small effects for $\mu_{2,3}\bar{R}_3 \gg 23$ [2,3]. Corrections due to the physical interaction range can be included through a two-body potential with two derivatives [14].

We use variational and diffusion Monte Carlo (VMC, DMC) methods for the solution of the Schrödinger equation. The trial-state wave functions are of the form

$$\Psi_T = \prod_i f^{(1)}(r_i) \prod_{i<j} f^{(2)}(r_{ij}) \prod_{i<j<k} f^{(3)}(R_{ijk}), \quad (4)$$

with $f^{(1)}(r) = \exp(-\alpha r^2)$, $f^{(2)}(r) = K \tanh(\mu_J r) \cosh(\gamma r)/r$, and $f^{(3)}(R) = \exp\{u_0 \exp[-R^2/(2r_0^2)]\}$. The parameters K and γ are chosen to have $f^{(2)}(d) = 1$ and $f^{(2)'}(d) = 0$ at the “healing distance” d . The variational parameters α , μ_J , d , u_0 , and r_0 are optimized at the VMC level for each system and interaction as described in Ref. [15], and $\alpha = 0$ to simulate uniform matter. The VMC wave function is then used as input for exact DMC calculations; see, for example, Ref. [16]. The calculated energies are exact subject to statistical and time-step errors that can be made arbitrarily small. Results for the energy are independent of the trial wave function, though statistical errors may be large for poor choices. Other properties are extrapolated from the VMC and DMC results, which we have tested using different trial wave functions. The extrapolation errors are very small, on the order of a few percent or less, similar or smaller than the reported statistical errors.

Clusters.—Clusters with six or fewer bosons have been studied extensively in the literature with an emphasis on Efimov physics [5–10], for a review see Ref. [17]. Slightly larger clusters with similar interactions have also been considered previously [18–21]. Universal behavior was found for small clusters up to $N \leq 15$. Nonuniversal behavior beyond this point was attributed to finite-range

effects. For sufficiently small range, it is expected that clusters will be universal and have a binding energy per particle,

$$\frac{E_N}{N} = \xi_B(N) \frac{E_3}{3}, \quad (5)$$

where $\xi_B(N)$ is a universal function of N .

In Fig. 1 we show results for clusters of up to 60 bosons for Hamiltonians with $\mu_2\bar{R}_3 = 46$ and 65, and compare to those of Ref. [18] for $N \leq 15$. These yield a trimer rms radius $\langle r_3^2 \rangle^{1/2} \approx 0.61\bar{R}_3$ for our finite-range Hamiltonians. We consider three-body interactions with different ratios of two- to three-body interactions ranges, $X_\mu \equiv \mu_3/\mu_2 = 0.5$, 0.75, and 1.0. Finite-range interactions will show nonuniversal effects when the range of two- or three-particle interactions becomes significant compared to the average interparticle distance. This can be seen in the results of Refs. [18,21] around $N = 15$, and also in our results corresponding to the more bound trimers (open symbols with $\mu_2\bar{R}_3 = 46$ in Fig. 1) for smaller X_μ . For $\mu_2\bar{R}_3 = 65$ the three sets of points with $X_\mu = 0.5$, 0.75, 1.0 agree within statistical errors. For $N = 4$ our result [$3E_4/(4E_3) = 3.5(1)$ for $\mu_2\bar{R}_3 = 65$ and $X_\mu = 1.0$] also agrees very well with the precise calculation of Ref. [8] [$3E_4/(4E_3) = 3.46$], suggesting that Efimov-related few-body physics is properly captured by our potential.

Studies of unitary bosons commonly employ a zero-range two-body interaction with three-body hard-core interaction of radius R_0 . That interaction has a fixed value of $\bar{R}_3/R_0 \approx 15.3$ [23], which can be compared to our $\mu_2\bar{R}_3 = 65$ and $\mu_3\bar{R}_3 = 32, 49, 65$ for $X_\mu = 0.5, 0.75, 1.0$. The zero-range two-body plus hard-core interaction

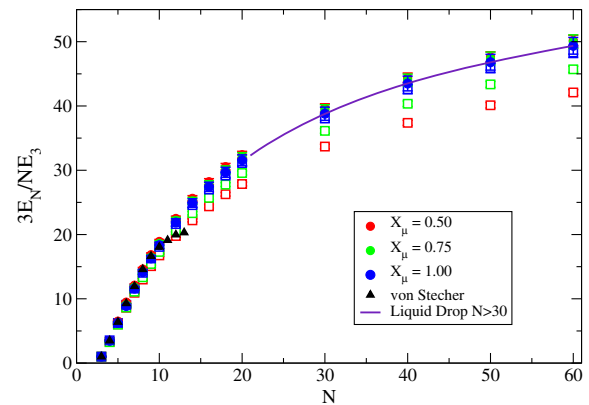


FIG. 1. Energy per particle of N -boson clusters scaled to the trimer energy per particle. Filled symbols are more loosely bound ($\mu_2\bar{R}_3 = 65$) and exhibit universal behavior (the results are also available in Ref. [22]); open symbols have larger two-body interaction range ($\mu_2\bar{R}_3 = 46$). Different colors indicate the ratio of two- to three-body interactions ranges, $X_\mu \equiv \mu_3/\mu_2 = 0.5$ (red), 0.75 (green), and 1.0 (blue). Results from Ref. [18] are indicated as (black) triangles. The solid (blue) line corresponds to a liquid-drop fit.

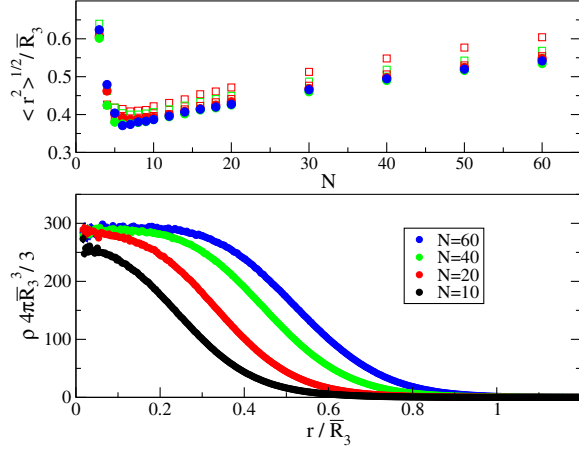


FIG. 2. Rms radii of N -boson clusters (upper panel) and radial one-body density of various clusters (lower panel), in units given by the three-boson distance scale \bar{R}_3 . Symbols in the upper panel are the same as for Fig. 1. In the lower panel, the curves with $N = 10$ (black), 20 (red), 40 (green) and 60 (blue) bosons are for $\mu_2 \bar{R}_3 = 65$ and $X_\mu = 1$.

can reproduce universal physics for small clusters but the three-body hard core is not small compared to typical near-neighbor separations for larger clusters ($N > 15$) or matter, as discussed below.

For small N the binding energy per particle increases approximately linearly with N , and by $N > 7$ it is an order of magnitude larger than the trimer's. Since we have tuned the trimer energy to be very small we can find universal behavior up to $N = 60$ clusters, as shown by the solid points ($\mu_2 \bar{R}_3 = 65$) in Fig. 1. For a 60-particle cluster the binding per particle is approximately 50 times that of the trimer. Naive dimensional arguments would suggest that the repulsive three-body interaction will become more important for large N , resulting in saturation to a constant binding energy per particle similar to what is observed in atomic nuclei. The energies per particle for large clusters are beginning to saturate to a constant value as shown in Fig. 1. Similar behavior has been seen in finite-temperature simulations in a trap [24,25].

We have also calculated the single-particle densities and radii of the N -particle clusters. Radii are also expected to scale with a universal ratio of the trimer rms radius: $\langle r_N^2 \rangle^{1/2} = \beta(N) \langle r_3^2 \rangle^{1/2}$. Results are shown in Fig. 2. The upper panel shows that the cluster radius reaches a minimum around $N = 5 - 7$, and then increases as saturation sets in. For larger clusters one would expect the radius to increase as $N^{1/3}$ for a system saturating to an equilibrium density. The lower panel shows single-particle densities for different particle numbers N and demonstrates the saturation of the single-particle density near the center of the clusters at a value independent of cluster size.

Matter.—We have also computed the properties of the bulk Bose liquid at unitarity for these same interactions using periodic boundary conditions. We expected very

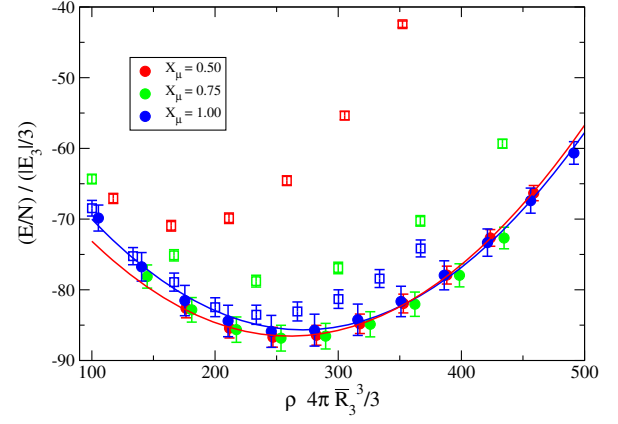


FIG. 3. Zero-temperature equation of state vs density for the unitary Bose fluid. Symbols as in Fig. 1. The two curves show quadratic fits around saturation density for $X_\mu \equiv \mu_3/\mu_2 = 0.5$ (red) and 1.0 (blue).

small finite-size effects, and confirmed this by comparing results for 20, 40, and 60 particles. Results for different N at the same density are equivalent within statistical errors. We find a universal equation of state (EOS) with an equilibrium ground-state energy per particle of 87 ± 5 times that of the trimer, and a saturation density of $\rho_0 4\pi \bar{R}_3^3 / 3 = 275 \pm 20$. The results are summarized in Fig. 3. Near saturation density they are well described by

$$\frac{3E_N(\rho)}{N|E_3|} \Big|_{N \rightarrow \infty} = \xi_B(N \rightarrow \infty) \left[-1 + \kappa \left(\frac{\rho - \rho_0}{\rho_0} \right)^2 \right], \quad (6)$$

with the dimensionless compressibility $\kappa = 0.42(5)$. The curves in Fig. 3 are fits to the EOS calculations with two different X_μ .

The calculations of the liquid are consistent with those obtained by extrapolating the cluster results. A liquid-drop extrapolation of the cluster binding energies, $E_N/N = E_B(N \rightarrow \infty)(1 + \eta N^{-1/3} + \dots)$, is consistent with the energies found for the bulk. Fitting results for $N > 30$, we find that the universal energy parameter $\xi_B(N \rightarrow \infty) = 90 \pm 10$. The surface energy scaled by the volume energy $E_B(N \rightarrow \infty)$ is $\eta = -1.7 \pm 0.3$, but has relatively large statistical errors. Similarly, the single-particle density near the center of the drops shown in Fig. 2 is consistent with the equilibrium density of matter. Despite the growth in energy with N , the liquid can be considered universal: the interparticle separation at equilibrium, $[3/(4\pi\rho_0)]^{1/3} \simeq \bar{R}_3/6.4$, is almost 4 times larger than the distance scale set by the next deeper Efimov trimer in the universal system without cutoffs. It is also 5–10 times larger than the two- and three-body interaction ranges, in contrast to ~ 2 for a zero-range two-body plus three-body hard-core interaction at the same density.

It is interesting to compare these results to liquid ^4He , which has a large two-body scattering length and, for small N , weakly bound clusters that can be described by

short-range interactions. Per particle, the binding energy of liquid ^4He is -7.14 K [26], which is about 180 times that of the ^4He trimer, -0.0391 K [27]. The scaled surface energy is ≈ -2.7 [27] and the dimensionless compressibility is ≈ 1.9 [26]. For small N the helium clusters are universal [28], but for large N the interaction range is comparable to the interparticle separation and hence not universal. Nevertheless, the ratio of binding energies $\xi_B(N \rightarrow \infty)$ and the scaled surface energy η are within a factor of 2 of unitary bosons.

We have also examined the two- and three-body contact parameters $C_{2,3}$ for the unitary Bose fluid at equilibrium density. These contact parameters impact various properties of the system, and relate the short-distance behavior to the high-momentum tail of the momentum distribution, see, for example, Refs. [29–33]. The two- and three-body distribution functions are shown in Fig. 4, normalized to one at large distances (differing by a factor of $\rho N!$ from the g_N defined in Refs. [31,32]).

In the universal regime outside the range of the interaction, the two-body distribution $g_2(r)$, with $r \equiv r_{ij}$, is expected to be proportional to $1/r^2$. The upper lines in the top panel show $32\pi^2\rho^{2/3}r^2g_2(r)/10$ for the different simulations, and the dashed line is a quadratic fit to results in the universal regime that can be extrapolated to $r = 0$ to give the dimensionless two-body contact α_2 , with $C_2 = N\alpha_2\rho^{4/3}$ [29]. From the extrapolation of r^2g_2 we find $\alpha_2 = 17(3)$. More accurate results may be achievable through simulations at different scattering lengths with fixed E_3 . This result is larger but qualitatively comparable

to those obtained in more approximate approaches [34] or those obtained with zero-range two-body plus hard-core three-body interactions [35,36], and quite similar to those extracted through rapid experimental quenches [29,30].

Similarly, in the bottom figure the dashed line is a fit to $g_3(r)$, with $r \equiv R_{ijk}$. In the universal regime, extrapolating to $r = 0$ gives the three-body contact. It is more accurate to extract the dimensionless three-body contact β_3 , with $C_3 = N\beta_3\rho^{2/3}$ [29], from the derivative of the energy with respect to \bar{R}_3 at constant scattering length. Using the equilibrium properties calculated in Fig. 3 we obtain $\beta_3 = 0.9(1)$. The density dependence of β_3 around equilibrium can be extracted from Eq. (6). Further simulations could yield the density dependence of α_2 , and also the asymptotic behavior of the momentum distribution g_3 .

With these strong correlations and the large binding and small radii relative to the trimer, one might expect that the condensate fraction may be reduced in the bulk. In fact we find quite a large condensate fraction at equilibrium density, with $n(k=0) = 0.93(1)$, compared to a value of unity for a weakly interacting Bose gas. One can also compare to liquid ^4He which has a condensate fraction of $0.0725(75)$ at equilibrium density [37].

The large condensate fraction implies that it is reasonable to access equilibrium properties of the universal Bose fluid as a function of density through experiments with rapid quenching of a weakly interacting gas [38,39]. The universal properties of the unitary Bose fluid are difficult to measure using standard techniques because of losses to deeply-bound three-body states that occur in cold atoms but are absent in our simulations. These loss mechanisms can lead to a trap lifetime smaller than that needed to reach full equilibrium, and presently available studies investigate this dynamics of the rapid quenching of the free-to-unitary transition. Our results indicate that a rapid quench from a weakly interacting Bose gas at the appropriate density may enable one to obtain the equilibrium properties. The relatively large overlap of the two states should lead to a rapid ejection of particles through high-energy two- and three-body processes, leading to a rapid cooling of the system. Quantifying this energy loss could lead to an experimental verification of the universal properties of the unitary Bose fluid in thermal equilibrium.

Summary.—We have demonstrated the universal nature of bosons at unitarity using short-range interactions tuned to unitarity in the two-body system and weak binding (Efimov) trimers in the three-body system. We have determined many of the universal properties of the unitary Bose fluid, including the energies and radii of clusters of up to 60 bosons and calculated the universal saturation and contacts of the unitary Bose fluid. We find a ground-state energy per particle of approximately 90 times that of the trimer at an associated high density. We find a large two-body contact parameter, yet the condensate fraction in the bulk is greater than 90%. We also calculate the three-body

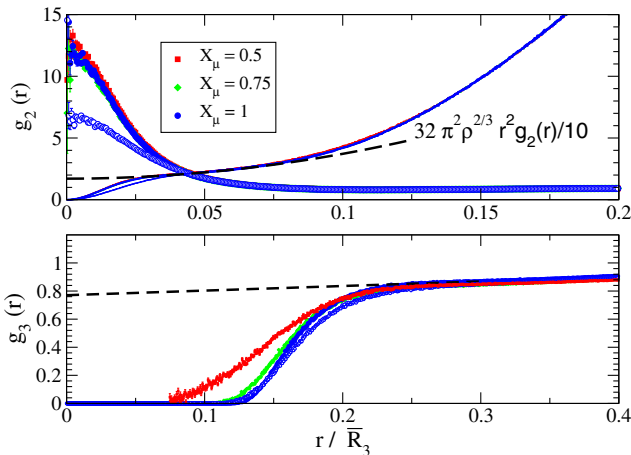


FIG. 4. Two- (upper panel) and three- (lower panel) body distributions in the unitary Bose fluid at saturation density, both normalized to unity at large separations. Symbols indicate simulations with different two- and three-body ranges, as in previous figures. For the two-body distributions in the upper panel, multiplying by r^2 allows an extrapolation (dashed line) to $r = 0$ to obtain the contact. In the lower panel, the three-body contact (dashed line) can also be extrapolated from the universal regime (dashed line) to $r = 0$.

contact parameter for the first time. Further experimental and theoretical studies of the unitary Bose fluid will be very intriguing. Many new properties can be studied, including those described above, collective effects and the static and dynamic response of the system.

We thank Daekyoung Kang for many valuable discussions. The work of J. C. and S. G. was supported by the NUCLEI SciDAC program, and by the U.S. DOE under Contract No. DE-AC52-06NA25396. The work of U. vK. was supported in part by the U.S. Department of Energy, Office of Science, Office of Nuclear Physics, under Award No. DE-FG02-04ER41338, and by the European Union Research and Innovation program Horizon 2020 under Grant Agreement No. 654002. S. V. thanks the hospitality and financial support from LANL and the facilities offered by CENAPAD-SP. Computational resources have been provided by Los Alamos Open Supercomputing. We also used resources provided by NERSC, which is supported by the U.S. DOE under Contract No. DE-AC02-05CH11231.

*carlson@lanl.gov

†stefano@lanl.gov

‡vankolck@ipno.in2p3.fr

§vitiello@ifi.unicamp.br

- [1] S. Giorgini, L. P. Pitaevskii, and S. Stringari, *Rev. Mod. Phys.* **80**, 1215 (2008).
- [2] P. F. Bedaque, H. W. Hammer, and U. van Kolck, *Phys. Rev. Lett.* **82**, 463 (1999).
- [3] P. F. Bedaque, H. W. Hammer, and U. van Kolck, *Nucl. Phys.* **A646**, 444 (1999).
- [4] L. H. Thomas, *Phys. Rev.* **47**, 903 (1935).
- [5] V. Efimov, *Phys. Lett. B* **33**, 563 (1970).
- [6] H. W. Hammer and L. Platter, *Eur. Phys. J. A* **32**, 113 (2007).
- [7] J. von Stecher, J. D’Incao, and C. Greene, *Nat. Phys.* **5**, 417 (2009).
- [8] A. Deltuva, *Phys. Rev. A* **82**, 040701 (2010).
- [9] M. Gattobigio, A. Kievsky, and M. Viviani, *Phys. Rev. A* **84**, 052503 (2011).
- [10] J. von Stecher, *Phys. Rev. Lett.* **107**, 200402 (2011).
- [11] E. Braaten and H. W. Hammer, *Phys. Rep.* **428**, 259 (2006).
- [12] J. Carlson, S. Y. Chang, V. R. Pandharipande, and K. E. Schmidt, *Phys. Rev. Lett.* **91**, 050401 (2003).
- [13] S. Y. Chang, V. R. Pandharipande, J. Carlson, and K. E. Schmidt, *Phys. Rev. A* **70**, 043602 (2004).
- [14] U. van Kolck, *Nucl. Phys.* **A645**, 273 (1999).
- [15] S. Sorella, *Phys. Rev. B* **64**, 024512 (2001).
- [16] W. M. C. Foulkes, L. Mitas, R. J. Needs, and G. Rajagopal, *Rev. Mod. Phys.* **73**, 33 (2001).
- [17] P. Naidon and S. Endo, *Rep. Prog. Phys.* **80**, 056001 (2017).
- [18] J. von Stecher, *J. Phys. B* **43**, 101002 (2010).
- [19] A. N. Nicholson, *Phys. Rev. Lett.* **109**, 073003 (2012).
- [20] A. Kievsky, N. K. Timofeyuk, and M. Gattobigio, *Phys. Rev. A* **90**, 032504 (2014).
- [21] Y. Yan and D. Blume, *Phys. Rev. A* **92**, 033626 (2015).
- [22] See Supplemental Material at <http://link.aps.org/supplemental/10.1103/PhysRevLett.119.223002> for additional data from specific simulations.
- [23] T. Comparin, <https://tel.archives-ouvertes.fr/tel-01411912/document> (2016).
- [24] S. Piatecki and W. Krauth, *Nat. Commun.* **5**, 3503 (2014).
- [25] T. Comparin and W. Krauth, *Phys. Rev. Lett.* **117**, 225301 (2016).
- [26] P. R. Roach, J. B. Ketterson, and C.-W. Woo, *Phys. Rev. A* **2**, 543 (1970).
- [27] V. R. Pandharipande, J. G. Zabolitzky, S. C. Pieper, R. B. Wiringa, and U. Helmbrecht, *Phys. Rev. Lett.* **50**, 1676 (1983).
- [28] B. Bazak, M. Eliyahu, and U. van Kolck, *Phys. Rev. A* **94**, 052502 (2016).
- [29] D. H. Smith, E. Braaten, D. Kang, and L. Platter, *Phys. Rev. Lett.* **112**, 110402 (2014).
- [30] E. Braaten, D. Kang, and L. Platter, *Phys. Rev. Lett.* **106**, 153005 (2011).
- [31] F. Werner and Y. Castin, [arXiv:1001.0774](https://arxiv.org/abs/1001.0774).
- [32] F. Werner and Y. Castin, *Phys. Rev. A* **86**, 053633 (2012).
- [33] S. Gandolfi, K. E. Schmidt, and J. Carlson, *Phys. Rev. A* **83**, 041601 (2011).
- [34] J. J. R. M. van Heugten and H. T. C. Stoof, [arXiv:1302.1792](https://arxiv.org/abs/1302.1792).
- [35] M. Rossi, L. Salasnich, F. Ancilotto, and F. Toigo, *Phys. Rev. A* **89**, 041602 (2014).
- [36] A. G. Sykes, J. P. Corson, J. P. D’Incao, A. P. Koller, C. H. Greene, A. M. Rey, K. R. A. Hazzard, and J. L. Bohn, *Phys. Rev. A* **89**, 021601 (2014).
- [37] H. R. Glyde, S. O. Diallo, R. T. Azuah, O. Kirichek, and J. W. Taylor, *Phys. Rev. B* **84**, 184506 (2011).
- [38] P. Makotyn, C. E. Klauss, D. L. Goldberger, E. A. Cornell, and D. S. Jin, *Nat. Phys.* **10**, 116 (2014).
- [39] R. J. Fletcher, R. Lopes, J. Man, N. Navon, R. P. Smith, M. W. Zwierlein, and Z. Hadzibabic, *Science* **355**, 377 (2017).